Crystallization of struvite in a hydrothermal solution with and without calcium and carbonate ions

by Athanasius Bayuseno

Submission date: 28-Aug-2021 01:32AM (UTC+0700)
Submission ID: 1636984841
File name: Chemosphere_250_2020.pdf (1.89M)
Word count: 9130
Character count: 49478

Chemosphere 250 (2020) 126245

Contents lists available at ScienceDirect

Chemosphere

journal homepage: www.elsevier.com/locate/chemosphere

Crystallization of struvite in a hydrothermal solution with and without calcium and carbonate ions

Athanasius P. Bayuseno [a, *], Wolfgang W. Schmahl [b]

[a] Center for Waste Management, Mechanical Engineering Graduate Program, Diponegoro University, Tembalang Campus, Semarang, Indonesia
[b] Department of Earth-and Environmental Sciences, Ludwig-Maximilian- University of Munich, Germany

HIGHLIGHTS

- Hydrothermal simulation of struvite with a variety of $Mg^{2+}/Ca^{2+}/HCO^{-}_{3}$ ratios.
- Biomineralization of struvite and Ca-phosphate occurs in the hydrothermal solution.
- Regulation of $Mg^{2+}/Ca^{2+}/HCO^{-}_{3}$ ratios minimize precipitation of calcium phosphate.
- The quality and quantity of struvite relates varying pH and $Mg^{2+}/Ca^{2+}/HCO^{-}_{3}$ ratios.

ARTICLE INFO

Article history:
Received 6 November 2019
Received in revised form
15 February 2020
Accepted 15 February 2020
Available online 17 February 2020

Handling Editor: Yongmei Li

Keywords:
MAP solution
Hydrothermal method
Phosphate recovery
Struvite: hydroxyapatite

ABSTRACT

Hydrothermal experiments with magnesium, ammonium, and phosphate (MAP) solution at a temperature of 120 ^{O}C for 24 h and pH (9 and 10), whilst effects of varying $Mg^{2+}/Ca^{2+}/HCO^{-}_{3}$ ratios on struvite crystallization were examined. The study was performed to investigate their effects on the quality and quantity of crystals using the XRPD Rietveld refinement and SEM method. Obviously, the struvite crystallization was inhibited through the forming of calcite, dolomite, hydroxyapatite, sylvite, and Mg-whitlockite under different pH conditions. In the absence of Ca^{2+} and HCO^{-}_{3} ions, struvite and dittmarite were formed at pH solutions (9 and 10). Struvite proportion reduced with pH (9 and 10) under $Mg^{2+}/Ca^{2+}/HCO^{-}_{3}$ ratios (1:1:1 and 2:1:1), and depleted under the $Mg^{2+}/Ca^{2+}/HCO^{-}_{3}$ ratio of 1:2:2. An obvious change in morphologies of crystals into nanosized particles was observed. Results of the low proportion of struvite for experiments with $Mg^{2+}/Ca^{2+}/HCO^{-}_{3}$ molar ratios may be a drawback for phosphate recovery.

1. Introduction

Recovery of valuable compounds such as ammonium and phosphate from wastewater can be implemented through "simple to use" hydrothermal method. Recently, the hydrothermal system is widely known to be simple, cost-effective and easy to set up (Jesse and Davidson, 2019; Xue et al., 2015). Moreover, the system is suitable for use of wastewater treatment because of their low energy consumption (low temperatures in the single-step process), reduction of environmental impact, production with the versatility of struvite in any form and size. Correspondingly the hydrothermal method is a realistic option for ammonium and phosphorus recoveries from wastewater in struvite. However, the treatment stage benefit of wastewater by the hydrothermal method is slightly offset by generating a new waste residue containing chlorides, water-soluble sulfate and alkali ions (Jesse and Davidson, 2019). Hence, a degree of compromise may be required in the selection of hydrothermal treatment due to the competition between the quality benefits of struvite for a slow-release fertilizer and producing other pollutants (Li et al., 2019). Nevertheless, it is envisaged that the large good-quality crystals and quantity of struvite can be achieved by the hydrothermal treatment (Zhu et al., 2019).

Hydrothermal treatment of wastewater through struvite ($MgNH_4PO_4 \cdot 6H_2O$) precipitation with magnesium addition has been proposed for recovering nutrient source from wastewater (Li et al., 2019). Accordingly hydrothermal synthesis of struvite has become a promising technology for wastewater treatments (e.g. municipal sewage, industrial wastewater, liquid manure) to recover

* Corresponding author. Center for Waste Management, Department of Mechanical Engineering, Diponegoro University, Tembalang Campus, Semarang, 50275, Indonesia.
E-mail addresses: apbayuseno@lecturer.undip.ac.id (A.P. Bayuseno), wolfgang.w.schmahl@lrz.uni-muenchen.de (W.W. Schmahl).

https://doi.org/10.1016/j.chemosphere.2020.126245
0045-6535/

calcium, phosphate and potassium (Gaterell et al., 2000; Munir et al., 2017; Sartorius et al., 2011). Furthermore the hydrothermal synthesis of struvite can be adopted in wastewater treatment for recovering phosphorus in a relatively pure, publicly acceptable and potentially commercial form (de-Bashan and Bashan, 2004). As compared to other methods of crystallization and synthesis, hydrothermal synthesis methodology can produce safely crystalline phases, which can be unstable at a higher temperature, toward new mineral less harmful for the humans and new environmentally friendly processes, provide benefits for deterring and avoiding water evaporation occurring in the single hydrothermal process with high energy-efficiency. The method is also desirable for the carbonization of sewage sludge leading to the stabilized solid product and can recreate a role as a final treatment step for sewage sludge disposal (Reißmann et al., 2018). Additionally, the potential untapped market for struvite as a slow fertilizer make this option feasible in parallel with the nutrient reduction achieved in the wastewater (Williams, 1998; Durrant et al., 1999). At this time, the purity and size of the recovered crystal have become a great concern in order to meet the required for agriculture when used as fertilizer, of which the particle aggregate should have strong bonding for subsequent handling (collection, transport and landfilling). Also, the morphology and homogenous particles have been considered as an important factor for the quality of industrial fertilizer (Rahman et al., 2014; Talboys et al., 2016).

Correspondingly, the hydrothermal method for wastewater processing has become intensive research, because it can potentially yield the struvite product of with homogenous particle, which is mainly required for a fertilizer product (Elliott et al., 2015; Shanmugam et al., 2017). The hydrothermal method has attracted more attention recently, as the appropriate method of struvite crystallization by generating large good-quality crystals and nanoparticles with control over their content and composition (McMillen and Kolis, 2016). It was suggested previously that 100 m^3 wastewater could be converted into 1 kg of struvite (Shu et al., 2006). If the wastewater on the world can be treated by struvite crystallization, 63,000 tons of P_2O_5 can be recovered. This value is equal to 16% of world phosphate rock consumption for mineral fertilizers, whereas phosphate rock is a non-renewable resource that would be depleted within the century. Moreover, 171 g struvite with the purity at least 95% can be produced from livestock wastewater per square meter without washing. Thus phosphate recovery from wastewater through the hydrothermal synthesis of struvite could be potential options (de-Bashan and Bashan, 2004). Specifically, pH and MAP (magnesium, ammonium, and phosphorus) molar ratio are operating conditions to influence of struvite formed in the aqueous solution, on which the pH basic of favorable struvite formation could be reached by adding KOH or NaOH (Babic-Ivancic et al., 2006; Bayuseno and Schmahl, 2018; Booker et al., 1999; Song et al., 2015).

Further quality of struvite (chemical purity and homogenous crystal size) produced by hydrothermal synthesis may be depending on the selection of the processing parameters including the typical design of their reactor (Bhuiyan et al., 2007; Rawn et al., 1937; Snoeyink and Jenkins, 1980). In particular, temperature and foreign ions present in the solution are operation conditions influencing the degree of success on struvite precipitation (Bouropoulos and Koutsoukos, 2000; Doyle et al., 2003; Hanhoun et al., 2011; Muryanto and Bayuseno, 2014; Stratful et al., 2001). Also, the operating temperature may influence the struvite decomposition during hydrothermal process (Bayuseno and Schmahl, 2018). In some cases, the increasing temperature leads to a rising precipitation rate of struvite (Perwitasari et al., 2017). Conversely, crystal nucleation and growth of struvite may be hindered by the presence of other competing ions such as calcium, chloride, carbonates, sulfates, nitrates, fluorides, and fluorosilicates in the solution, which can determine the precipitation reaction and eventually the crystal quality (Abbona et al., 1986; Doyle and Parsons, 2002; Mohajit et al., 1989; Perwitasari et al., 2017). Also, the crystal shape of struvite with possible particle agglomeration may be altered by the presence of those competing ions (Booker et al., 1999; Ohlinger et al., 1999). It has been demonstrated previously that interaction of calcium, phosphate, or carbonate ions in the solutions may produce calcium phosphate hydrate (hydroxylapatite) and calcium carbonate as follows (Le Corre et al., 2005):

$$5Ca^{2+} + 3PO_4^{3-} + H_2O \rightarrow Ca_5(PO_4)_3OH + H^+ \quad pKsp = 54.45 \quad (1)$$

$$Ca^{2+} + HCO_3^- \rightarrow CaCO_3 + H^+ \quad pKsp = 6.40 \quad (2)$$

where pKsp is solubility product constants in form of - log10 Ksp at 25 °C. Hydroxyapatite has a higher solubility product constant than that of calcium carbonate indicating the more soluble compound in hydrothermal solution, and it may be precipitated depending on the alkalinity and supersaturation (Ajikumar et al., 2005). However, calcium carbonate ($CaCO_3$) has a lower solubility product constant, it may be easily precipitated in forms of either calcite (pKsp = 8.48), aragonite (pKsp = 8.34) or vaterite (pKsp = 7.91).

Instead of hydroxylapatite, magnesium phosphate compounds alongside struvite may be also formed with the variable of Mg^{2+}/Ca^{2+}/HCO^-_3 ratios in the solution, leading to retardation of the crystallization of hydroxylapatite (Le Corre et al., 2005; Liu and Wang, 2019). This is because the Ca-ion may control struvite formation in the solution, whereas the phosphate ions would compete or interfere with the crystallization of struvite. Moreover, carbonate ion available in the solution makes the hindrance of struvite precipitation and eventual changes in the characteristics of its crystal. Correspondingly, the concentration of phosphate, magnesium and calcium ions together with pH solution can play key role in the precipitation of magnesium and calcium phosphate, which influence the purity of the struvite product (Hii et al., 2014; Kofina et al., 2007; Kofina and Koutsoukos, 2003; Stratful et al., 2001). Therefore, an understanding of the controlled competitive ions in the hydrothermal solution is needed for achieving successful and economic processes at a full-scale, pilot-scale and bench-scale constructed wastewater treatment, in which the quality and quantity of struvite product are primarily concerned.

Generally, struvite may be grown in various mother solutions such as artificial urine, wastewater, and hydrothermal solution (Bhuiyan et al., 2008; Bouropoulos and Koutsoukos, 2000; Capdevielle et al., 2013; Doyle and Parsons, 2002). Specifically, the hydrothermal solution may contain hot waters in the temperature range of 50–300 °C, while processing parameters (e.g. supersaturation and concentration of chemical additives) are determining factor for crystallization of struvite and other phosphate-bearing minerals (Munir et al., 2017; Tansel et al., 2018). Accordingly, Ca^{2+} and HCO_3^- ions available in the hydrothermal solution may affect the nucleation and crystal growth of struvite (Le Corre et al., 2005; Korchef et al., 2011).

Much study has been undertaken to investigate different properties of struvite derived from a variant solution composition, however, only limited data on the mineralogical compositions of the struvite-mediated hydrothermal solution can be found in the literature, while the effects of Ca^{2+} and HCO_3^- ions and temperature on the crystallization of struvite in the hydrothermal solution have been not analyzed in depth. Here the chemical equilibrium modeling and material characterization experiments are required for providing complete data of the phase compositions of the product derived from the hydrothermal solution (Lu et al., 2016;

Bayuseno and Schmahl, 2018).

In the study, the struvite-containing precipitates were produced using a hydrothermal autoclave reactor of the MAP solution with variable $Mg^{2+}/Ca^{2+}/HCO^{-}_{3}$-ratios and pH, while the resulting precipitates were then examined in terms of purity and morphology of the crystals. The objective of the study was to design synthetic wastewater and evaluate the effects of Ca^{2+}/HCO^{-}_{3} on characteristics of hydrothermal precipitates based on the chemical modeling analysis and material characterization experiments. Together with X-ray powder diffraction (XRPD) and SEM analysis, scientific knowledge of struvite crystallization by the hydrothermal method will get insight into the effective treatment of wastewater for recovery of phosphate resource.

2. Materials and method

2.1. The prepared hydrothermal solution

A batch of hydrothermal experiments on struvite crystallization was carried out on the MAP solution prepared by the powders of magnesium chloride (0.025 M $MgCl_2$) and ammonium phosphate (0.025 M $NH_4H_2PO_4$) with the analytical grade of the chemical product (VWR Chemicals, Germany). Each powder was initially diluted with water into a glass beaker (500 ml volume), on which each resulting solution was then mixed in the glass beaker placed on a magnetic stirrer to produce stock MAP solutions with the molar ratio of 1:1:1. Moreover, powders of $CaCl_2 \cdot 2H_2O$ (Sigma-Aldrich) and $KHCO_3$ (Merk-Darmstadt) were added to the stock solution in order to provide molar ratios (1:1:1; 2:1:1 and 1:2:2) of $Mg^{2+}/Ca^{2+}/HCO^{-}_{3}$. A solution of 50% w/w KOH (Merck) was prepared and used to adjust the pH solution (9 and 10) during stirring at 60 rpm with the magnetic stirrer for 20 min until a white colloidal suspension was obtained. Moreover, a Teflon lined hydrothermal synthesis reactor with 50 ml capacity was filled by 80% of the total volume of the reactor with the precursor suspension. Heating of the reactor was performed in an electrical furnace to the desired temperature of 120 ^{O}C for 24 h. In this condition, the generation of autogenous pressure occurred within the autoclave-closed reactor, in which water evaporation could be avoided leading to bicarbonate keep at the same concentration in the solution. Hydrothermal process may also involve the carbonization of the solution, yielding the stabilized solid product, thereby acting as a final treatment step for the slurry disposal. After heating to the required time, the autoclave was slowly cooled within the furnace to room temperature. The reactor was then opened, while the obtained precipitates were withdrawn by filtering using a 0.22 μm filter paper (Wattman) and followed by washing several times with aquades for removing salt and the precipitating solid was then dried in a desiccator at room temperature for at least 24 h.

In this study, the experimental work was designed on a direct alkaline hydrothermal activation, in which KOH was added in the prepared hydrothermal solution in a closed autoclave reactor and heated at fixed temperature and time. Alkali metal hydroxide solutions were employed to activate the hydrothermal reactions because it has been shown to be effective in the struvite crystallization (Bayuseno and Schmahl, 2018). At the temperature of 120 ^{O}C, heating of the mixtures undertaken in the sealed conditions may yield most of the ammonia, if not all, was transformed into NH_3 species resulting from dissolution. However, the closed system of hydrothermal reactor can avoid NH_4^+ volatilization. Further hydrothermal condition at 120 ^{O}C provided the orthophosphate activity increasing in the excess water, implying that minerals other than struvite may be developed (Stum and Morgan, 1970).

Additionally, the heating rate of the hydrothermal reactor has a substantial role in the performances of struvite production. A literature review on each of the phosphate minerals provided a possibility of minerals formed in the period of time, while subsequent mineral stabilities could be influenced by the rate of heating and cooling of the reactor (Bhuiyan et al., 2008; Kontrec et al., 2005). For instance, struvite and dittmarite can be crystallized in a short period of time, and subsequent decomposition of those minerals may result from the slow hydration in the solution (Montes et al., 2009). Hydroxyapatite might be also formed from a hydrothermal synthesis of transforming slurries, solutions or gels under mild reaction conditions typically below 350 ^{O}C. Correspondingly the thermal stability, phase transition and decomposition of the products from the hydrothermal system would provide a better knowledge for engineering of struvite crystals and effects of reaction conditions on crystal quality.

2.2. Material characterization of the hydrothermal product

For the XRPD measurement, a sample holder with capillary glass tube (diameter = 0.5 mm) was filled-up by the dried powder and then exposed to an x-ray beam on an STOE-diffractometer (Germany) in transmission (Debye-Scherrer) geometry. The XRPD data were analyzed for phase identification by a search-match program using the MATCH software. Furthermore, the phase compositions of the hydrothermal product was determined by the Rietveld method with the Program Fullprof-2k, version 3.30 (Rodriguez-Carvajal, 2005). The Rietveld refinement program used the crystal structure model obtaining from the referenced crystal structure model (American mineralogist of crystal structure database -AMCSD) (Downs and Hall-Wallace, 2003).

So far the use of the conventional XRD method has a restriction in that some X-ray diffraction peaks in the diffractogram of multiple mineral phases having significant overlapped peaks could not be accurately identified. However, the drawbacks of superimposed peaks in traditional XRD analysis could be solved by the application of the Rietveld full profile fitting analysis (Rietveld, 1969; Mahieux et al., 2010; Perwitasari et al., 2017; Winburn et al., 2000). The Rietveld method was chosen in the study because: (i) quantitative data for major-minor phases were required, (ii) significant (sometimes total) overlapping peaks were found in samples, and (iii) best confidence in the reliability of result was needed. Here the Rietveld method relies on well known-crystal structure database for phases of natural and synthetic materials. In particular, high-resolution powder diffraction using a Debye-Scherrer transmission geometry was selected to provide better analytical XRD data for avoiding the generation of preferred orientation on the crystalline samples of the hydrothermal product.

The calculation for the contents of various minerals was performed using the refined scale factor of the Rietveld method using the Full-prof software to provide the relative weighted fractions of each mineral composition. In this method, the amounts of all phases present in the sample could be quantified simultaneously. The phase quantification procedure involved the identification of major and minor phases. Correspondingly total of (wt.%) the relative weighted fractions of the crystalline phases would be 100%.

Further dried powder samples were investigated by SEM technique for the crystal morphology identification. In this manner, the samples were placed on the Al-stubs using double-sided conductive tapes, and the powder surface was coated with carbon.

2.3. Chemical equilibrium modeling of minerals

The hydrothermal process of the synthetic solution may produce the particular minerals (e.g. struvite and hydroxyapatite), which could be simulated under varying $Mg^{2+}/Ca^{2+}/HCO^{-}_{3}$ ratios by the AQION software program (version 3.0). AQION is a free

hydrochemistry and water analysis software that can be used for validating aqueous solutions such as charge balance and (Electrical Conductivity) EC, calculating pH (acid-base reactions, addition of chemicals). This program uses the well-known U.S.G.S. software PhreeqC as an internal numerical solver (Parkhurst and Appelo, 1999). This software can connect the gap between scientific software and the calculation/handling of "simple" water-related tasks in daily routine practice.

In this way, the ionic strength calculation used the Davies activity coefficient approximation. Subsequently, the saturation index (SI) of each mineral was determined based on the calculation of software as:

$$SI = \log (IAP/Ksp) \quad (3)$$

Where IAP is the ion activity product and Ksp is the solubility product of MAP. In this calculation, an unsaturated condition occurs if SI < 0, on which there is no precipitation of minerals from the solution. Conversely, the spontaneous mineral precipitation would occur if the SI value is more than 0. In this study, the SI calculation for potential minerals precipitated from the hydrothermal solution is listed in Table 1. Further relative supersaturation was calculated using the speciation program of AQION. The AQION program has inbuilt solubility products for various relevant minerals and additional mineral constants (solubility products) used for the equilibrium calculation (Table 2). The solution pH was varied for different simulations at a constant temperature. Chlorine or sodium ion concentration was also allowed to vary to balance the charge of the solution. Here, pH values (9 and 10) and temperature of 120 ^{O}C were selected as the input parameters.

In general, struvite can favourably precipitate from high pH values (basic) and temperatures in various mother solutions (artificial urine or in artificial wastewater) (Bouropoulos and Koutsoukos, 2000; Doyle and Parsons, 2002). In particular, hydrothermal treatment of wastewater can effectively transport nutrient components in sewage sludge into the liquid product. Thus the hydrothermal method was adopted in this experimental study because of having great potential in the development of morphology-controlled nanomaterials for P recovery from the solution. Also, the method operates at low temperatures in the one-step process, thereby consuming the low energy. Practically, the advantages of the method can reduce environmental impact, produce versatility of many new minerals in any shape and size (Reißmann et al., 2018). Here, the choice of parameter ranges (pH value and temperature) was guided by the outcome of the previous hydrothermal experiments (Bayuseno and Schmahl, 2018) and this condition was considered still realistic for an economically feasible process of wastewater in struvite.

3. Results and discussion

3.1. Prediction for minerals formed in hydrothermal solution

Minerals precipitated from the hydrothermal solution could be predicted using the SI values, that are calculated by the AQION software based on the input data of Table 1. The calculated SI values in the program for providing the possibility of the mineral precipitation are then presented in Table 2. Correspondingly, minerals are likely to precipitate during the hydrothermal reaction relating to a positive SI value. In the varying pH solution examined in the study, struvite crystallization occurred depending on the variable MAP ratio, and also may be affected by the variation of $Mg^{2+}/Ca^{2+}/HCO^{-}_{3}$ ratios (Bouropoulos and Koutsoukos, 2000; Ohlinger et al., 2000 Bouropoulos and Koutsoukos, 2000; Ohlinger et al., 2000). Accordingly, in the absence of Ca^{2+} and HCO^{-}_{3}, struvite crystallization is preferable in the hydrothermal solution with the MAP molar ratio of 1: 1: 1 at the working temperature of 120 ^{O}C and pH solution of 9 and 10. In addition to struvite, the two main magnesium phosphate compounds (i.e. bobierrite and cattite) may precipitate during the hydrothermal process. However, the possibility of those mineral formations depends on the hydrothermal operating conditions (Bayuseno and Schmahl, 2019). In some cases, bobierrite and cattite may precipitate very slowly, since their crystallization processes take time, therefore, they may be not formed in a hydrothermal process observed in the study (Mamais et al., 2012). Moreover, brucite [$Mg(OH)_2$] may be precipitated at a high pH solution (>9.5) (Musvoto et al., 2000a).

Further, pH solution of 9 and 10, and the presence of Ca^{2+} and

Table 1
The chemical composition of the hydrothermal solution.

No	Ion	Mg:NH_4:PO_4 (1:1:1) (mg/l)	Mg: Ca: HCO_3 (1:1:1) (mg/l)	Mg: Ca: HCO_3 (2:1:1) (mg/l)	Mg: Ca: HCO_3 (1:2:2) (mg/l)
1.	Mg	607.6	607.6	1215.2	607.6
2.	NH_4	450.9	450.9	450.9	450.9
3.	PO_4	2374	2374	2374	2374
4.	K	1742	1839.7	1839.7	1937.1
5.	Ca		1002	1002	2004
6.	Cl	1772.6	1772.6	3545.2	1772.6
7.	HCO_3		15524.2	15524.2	31048.4

Table 2
Mineral species with calculated SI of the hydrothermal solution.

Mineral species	Chemical Formula SI > 1	MAP ratio of 1:1:1		Mg:Ca:CO_3 ratio of 1:1:1		Mg:Ca:CO_3 ratio of 2:1:1		Mg:Ca:CO_3 ratio of 1:2:2	
		pH 9	pH 10	pH 9	pH 10	pH 9	pH 10	pH 9	pH 10
Bobierrite	$Mg_3(PO4)_2{\cdot}8H_2O$	5.55	5.77	8.58	8.19	7.037	6.660	7.11	8.06
Brucite	$Mg(OH)_2$	6.86	7.32	5.14	6.29	7.210	7.830	7.08	6.38
Calcite	$CaCO_3$			3.46	3.73	3.467	3.368	3.98	3.98
Cattiite	$Mg_3(PO_4)_2{\cdot}22H_2O$	3.38	3.35	6.14	5.71	4.496	4.036	4.55	5.55
Dolomite	$CaMg(CO_3)_2$			6.38	7.74	7.481	7.232	8.27	8.46
Hydroxyapatite	$Ca_5(PO_4)_3OH$			19.24	24.24	22.23	24.33	25.49	25.62
Magnesite	MgCO3			2.86	4.2	3.870	3.814	4.24	4.43
Struvite	$MgNH_4PO_4{\cdot}6H_2O$	3.15	2.21	0.16	2.18	1.129	0.613	1.23	2.06

HCO^{-}_{3} promoted the growth of hydroxylapatite and calcite, which possibly precipitate with struvite. Calcite is the more stable phase at room temperature, which favorable precipitate in alkaline environments. However, Mg^{2+}, phosphate, and dissolved organics present in the solution may control the calcium carbonate precipitation (Musvoto et al., 2000a). Therefore, magnesite ($MgCO_3$) possibly form in a pH range of less than 10.7, and, its formation may occur in the hydrothermal solution (Musvoto et al., 2000b). Also, dolomite and brucite may be found as a precipitate at high pH (>9.5) (Musvoto et al., 2000b).

Among different calcium phosphate compounds, hydroxyapatite may be formed, while amorphous calcium phosphate (ACP, $Ca_3(PO4)_2(xH_2O)$ may be formed during hydrothermal process and then possibly decomposed to hydroxyapatite (Abbona et al., 1986). Additionally, bobierrite and cattiite are suggested to precipitate in the supersaturated solution containing Ca^{2+} and HCO^{-}_{3} ions (Bouropoulos and Koutsoukos, 2000; Ohlinger et al., 2000). The SI calculation results of the calcium-carbonate containing hydrothermal solution would be judged by the XRPD Rietveld method for qualitative and quantitative phase compositions of the hydrothermal products.

3.2. Quality of the hydrothermal product

Dry precipitates resulted from the hydrothermally-generated solution in the absence of Ca^{2+} and HCO^{-}_{3} ions were evaluated by a qualitative XRPD method. In this way, search-matched by XRPD patterns was done with the mineral database from the standard powder diffraction database (PDF) of the International Centre for Diffraction Data (ICDD) (PDF-2, ICDD-Release, 2008). Here, dittmarite (PDF#36−1491) and struvite (PDF#71−2089) were matched with the database in addition to sylvite (PDF#73−0380). On the basis phase identification results, the Rietveld refinement of the XRPD data confirmed that struvite and dittmarite were precipitated by the hydrothermal process at the temperature of 120 ^{O}C and pH of 9, while sylvite was found possibly during drying the sample (Fig. 1a). It shows that the Rietveld refinement has a good agreement between the observed (Yobs) and calculated diffraction patterns (Ycalc) which indicates the high quality of phase identification. The obtained value for a GOF (goodness of fit) of 1.215 is also close to 1, therefore phase composition analysis in the precipitates was deemed to be acceptable quality.

Fig. 1b shows XRPD outcomes of hydrothermal synthesis at varying pH of 9 and 10. Dittmarite, struvite, and sylvite represent the hydrothermal product precipitated at a temperature of 120 ^{O}C. The outcome of synthetic lab-made hydrothermal minerals could be considered quite accurate, since dittmarite, struvite and sylvite peaks have been judged by the Rietveld method close in agreement with the literature data (Bayuseno and Schmahl, 2018). In this case, the precipitation of dittmarite could not be presented in the AQION program, but the finding could be confirmed by XRPD method. The reason reflects the solubility of dittmarite closed to the struvite (Bhuiyan et al., 2008; Doyle et al., 2002). Dittmarite may be formed due to the orthophosphate activity increased in the excess water (Bhuiyan et al., 2008), which also depends on the operating condition and subsequent cooling to room temperature (Bayuseno and Schmahl, 2018).

Further investigation of the sample precipitated at pH 10 provided no difference in mineralogy phase composition. Here, struvite and dittmarite crystals were still observed, while pH and temperature are not significant parameters controlling the quality of the hydrothermal product (Bhuiyan et al., 2008; Musvoto et al., 2000b). The previous study identified the mechanisms via supersaturation and ammonia activity in the solution, which struvite precipitated and subsequent partially transformed into dittmarite after heating the hydrothermal reactor containing solution with pH 9 and 10 at 120 ^{O}C (Bayuseno and Schmahl, 2018). Additionally, a few crystals such as bobierrite and cattiite could not be detected by the XRPD method, although they may be formed in this range pH as suggested by the AQION program. The reason for not-finding for those minerals is linked to their crystallization time as supposed to happen in the order of days or months (Musvoto et al., 2000b). Likewise, the kinetics of any crystal growth could not be predicted by the AQION program.

Furthermore, XRPD analysis of the hydrothermal product showed patterns with the broadening of peak size and background noise were observed from the precipitates with the $Mg^{2+}/Ca^{2+}/HCO^{-}_{3}$ ratio of 1:1:1 (Fig. 2a). Results indicated that a glassy phase formed in the samples in addition to the microcrystalline phases. Though the Rietveld refinement had some difficulties on

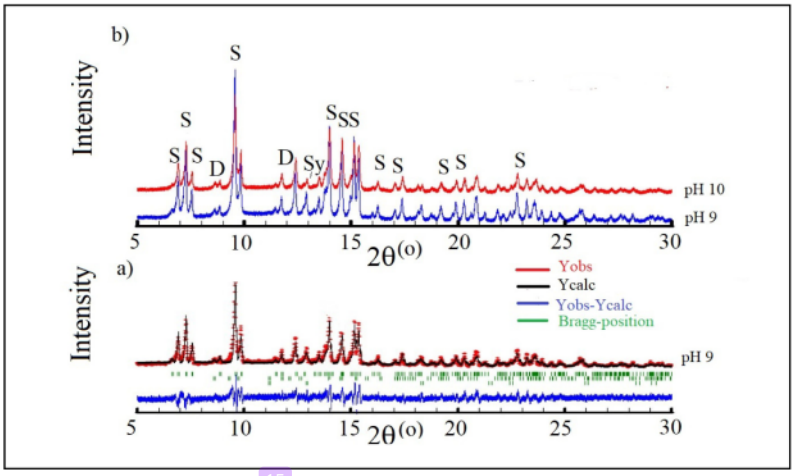

Fig. 1. a) XRPD Rietveld refinement plot of the hydrothermal product at pH 9 with MAP ratio of 1:1; 1, b) XRPD patterns of the samples precipitated at varying pH of 9 and 10. Notes: dittmarite (D), struvite (S) and sylvite (Sy), respectively.

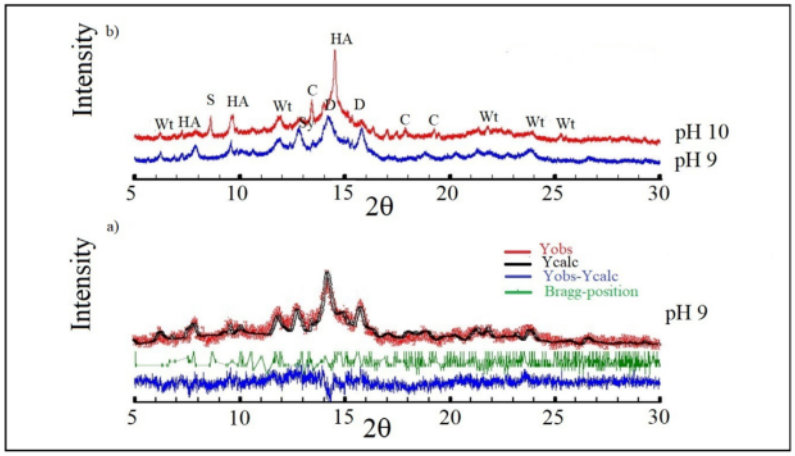

Fig. 2. a) XRPD Rietveld refinement plot of the hydrothermal product in the presence of Ca and HCO_3; b) XRPD pattern of the samples precipitated from the hydrothermal solution with ionic molar ratio of Mg, Ca and HCO_3 (1:1:1) and different pH of 9 and 10. Notes: calcite (C); dolomite (D); hydroxyapatite (HA); struvite (S); sylvite (Sy); Mg-whitlockite (Wt), respectively.

determination of profile and background functions, calcite (C), dolomite (D), hydroxyapatite (HA); struvite (S); sylvite (Sy) and Mg-whitlockite (Wt) [$Ca_9Mg(PO_4)6PO_3OH$] were confirmed to form at pH 9.0 and 10. Apparently, both hydroxyapatite and Mg-whitlockite formed to be related by the binding of their constituting ions, in which magnesium may render hydroxyapatite originating from amorphous calcium phosphate (Liu and Wang, 2019).

Correspondingly, all XRPD Rietveld refinements were considered to be acceptable quality, on which there was in a close agreement between the observed (Yobs) and the calculated (Ycalc) intensities. Obviously, the presence of Ca^{2+} and HCO^{-}_3 ions was significant to affect all diffraction peaks of phosphorus in the XRPD spectra (Le Corre et al., 2005). Consequently, the formation of other crystalline phases leads the overlapped peaks in the XRPD patterns (Fig. 2b), while the peak intensity of struvite was shown to reduce.

At $Mg^{2+}/Ca^{2+}/HCO^{-}_3$ mole ratio of 2:1:1 and pH of 9, the hydrothermal products are composed of calcite, hydroxyapatite, struvite, and sylvite, which can be observed by the plot of the XRPD refinement outcome (Fig. 3a). Similar to pH 10, the hydrothermal product consisted of XRPD profile peaks that correspond with the standard profile pattern for calcite, hydroxyapatite, struvite, and sylvite (Fig. 3b). In the presence of Ca^{2+} and HCO^{-}_3 ions, calcite can be obviously formed in the product, while hydroxyapatite can precipitate at pH 9 and above. Apparently, struvite precipitation was hindered by the development of hydroxyapatite depending on the $Mg^{2+}/Ca^{2+}/HCO^{-}_3$ mole ratio (Yan and Shih, 2016).

Subsequent struvite crystallization was examined by XRPD Rietveld analysis on the samples precipitated at a pH of 9 and 10 with the $Mg^{2+}/Ca^{2+}/HCO^{-}_3$ ratio of 1:2:2 (Fig. 4). The XRPD Rietveld analysis of the sample precipitated at pH 9 indicated that there was no struvite formed and replaced by precipitation of

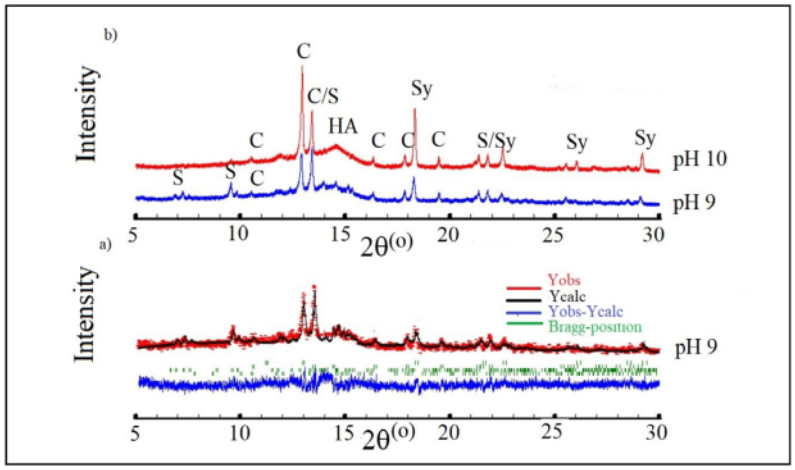

Fig. 3. a) XRPD Rietveld refinement plot of hydrothermal product in the presence of Ca and HCO_3 at pH 9; b) XRPD pattern of the samples precipitated from the hydrothermal solution with ionic molar ratio of Mg, Ca and HCO_3 (2:1:1) and different pH of 9 and 10. Notes: calcite (C); hydroxyapatite (HA); struvite (S); sylvite (Sy), respectively.

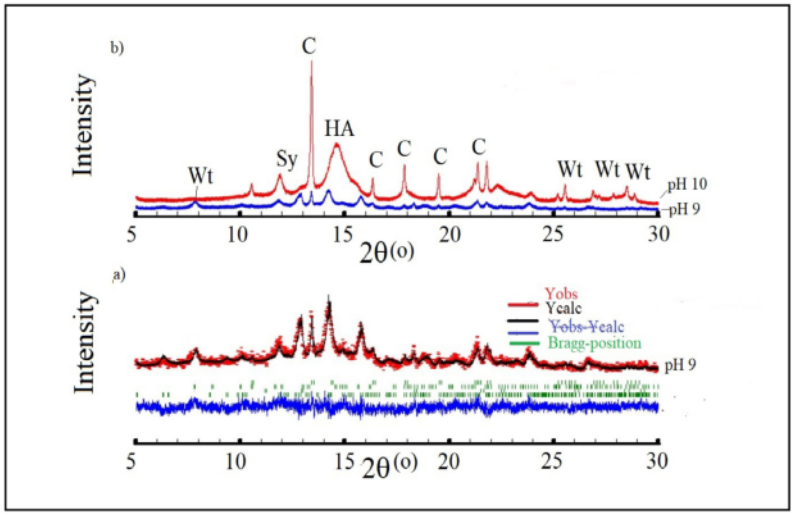

Fig. 4. a) XRPD Rietveld refinement plot of hydrothermal product in the presence of Ca and HCO_3; b) XRPD pattern of the samples precipitated from the hydrothermal solution with ionic molar ratio of Mg, Ca and HCO_3 (1:2:2) and different pH of 9 and 10. Notes: calcite (C); hydroxyapatite (HA); struvite (S); sylvite (Sy); Mg-whitlockite (Wt), respectively.

hydroxyapatite and Mg-whitlockite (Fig. 4a). These results are consistent with the finding of the Ca^{2+}/Mg^{2+} ratio of 2:1 as the most favorable environment for calcium phosphate compounds crystallization under this hydrothermal condition (Liu and Wang, 2019; Yan and Shih, 2016). When the pH is higher than 9.0, only hydroxyapatite was precipitated from the hydrothermal solution. In addition to interference from Ca2+ and HCO-3 ions, calcite formed and controlled struvite formation at pH 10. Correspondingly, the XRPD intensity peak was observed to have a larger HA peak characterized by a larger peak situated at 2θ of 14.446°.

Further, morphology evaluation on the quality of struvite formed from the hydrothermal process was performed by scanning electron microscopes (SEM). The SEM images of the morphology of the sample obtained from the hydrothermal solution of pH 9 and 10 are given in Fig. 5. A typical irregular prismatic shaped morphology of struvite could be observed in the samples (Fig. 5a, c), similar to the previous encounter of struvite morphology precipitated at the solution pH range of 7–11 (Bayuseno and Schmahl, 2018; Bouropoulos and Koutsoukos, 2000; Ohlinger et al., 2000). Moreover, SEM analysis supported the results of the XRPD Rietveld method that the crystallization of struvite and dittmarite was subsequently influenced by the presence of Ca^{2+} and HCO^{-}_{3} ions. In the absence of those ions in the solution, the regular shape of the struvite morphology could be distinguished but covered by a precipitate (Fig. 5a, c). However, the hydrothermal product obtained at the ratio of Mg^{2+}/Ca^{2+} of 1:1, showing the small crystals that were associated with a larger plate-like crystal (Fig. 5b, d). This result supported the hypothesis that the crystallization of struvite is inhibited, instead yielding to the formation of an amorphous phase, probably the calcium phosphate compound. Moreover, another phase could be developed with struvite, hence resulting in a change of morphology. Likewise, for experiments undertaken with varying molar Mg^{2+}/Ca^{2+} ratio, though not shown in this paper, the morphology including size and shape of struvite changed as more molar Mg^{2+}/Ca^{2+} ratio available in the solution to form large crystal aggregates surrounded by the small microcrystalline. Also, pH was not significantly influencing the change of morphologies. All of the products obtained from the hydrothermal solution with the variable of $Mg^{2+}/Ca^{2+}/HCO^{-}_{3}$ have irregular shape morphology with small size (<5 μm) (see-Figure 5b, d).

3.3. Impacts of calcium and carbonate ions on quantity of the hydrothermal product

Whereas morphology and purity are important parameters for struvite recovery of the hydrothermal process, the quantity of the mineral product can be considered as an indicator of the economic viability of the hydrothermal process. In the study, the phase compositions of the hydrothermal products were analyzed by quantitative Rietveld method. The XRPD phase quantification results in the precipitates at varying $Mg^{2+}/Ca^{2+}/HCO^{-}_{3}$ molar ratios of the hydrothermal solution are presented in Table 3 including the solubility product constants of all minerals. However, the solubility product constant for dittmarite is not available in the literature, however, it was suggested that its value is close to that of struvite (Bhuiyan et al., 2008). According to the constant values, most minerals identified by the XRPD method were proposed to be precipitated by the hydrothermal method observed during the study, instead of sylvite which may be formed after drying the samples.

Further content of struvite in the precipitates above 90 wt % could be produced from the hydrothermal solution in the absence of Ca^{2+} and HCO^{-}_{3}-ions. However, its content reduced with a pH of 10. Accordingly, dittmarite has become a minor phase instead of sylvite. When the ratios of $Mg^{2+}/Ca^{2+}/HCO^{-}_{3}$ were 1:1:1 or higher, the precipitates contained struvite below 50 wt % or less. The reason for the lower production of struvite is related to the presence of those competitive ions including pH solution (pH = 10). Apparently, struvite production (wt. %) has a correlation of the $Mg^{2+}/Ca^{2+}/HCO^{-}_{3}$ molar ratios. As a significant concentration of $Mg^{2+}/Ca^{2+}/HCO^{-}_{3}$ ions existed in the solution, calcium ion may be formed in hydroxyapatite and calcite crystals, while Mg-whitlockite may be developed relating to the higher ratio of Ca^{2+}/Mg^{2+} (2:1).

3.4. Significant outcomes of hydrothermal experiments

The laboratory experiments with varying $Mg^{2+}/Ca^{2+}/HCO^{-}_{3}$

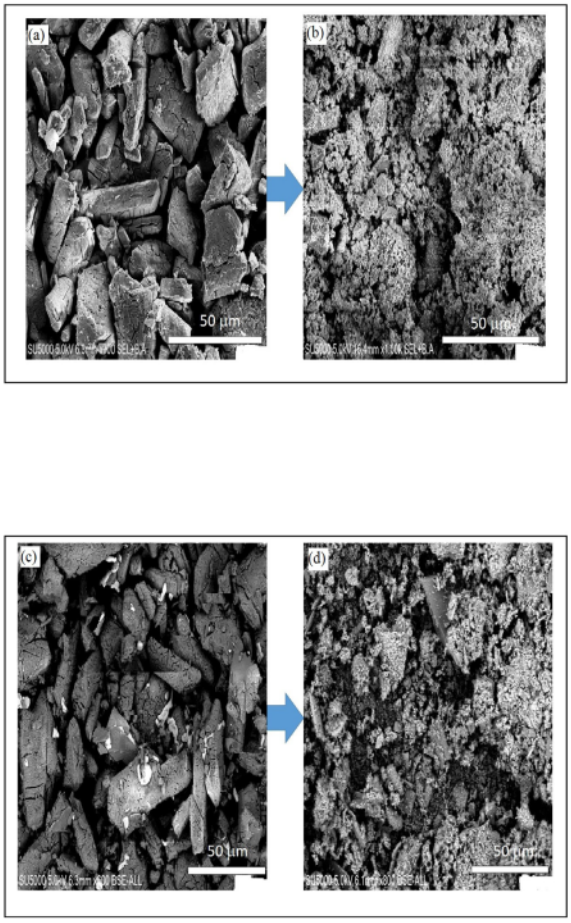

Fig. 5. SEM image of morphology crystals precipitated from the hydrothermal solution at a) pH of 9 in the absence of Ca and HCO_3-ions; b) pH of 9 with the molar Mg: Ca: HCO_3 of 1:1:1; and c) pH 10 in the absence of Ca and HCO_3-ions and d) pH 10 with the molar Mg: Ca: HCO_3 of 1:1:1 respectively.

molar ratios and pH solution of struvite precipitation at the batch hydrothermal reactor have significant outcomes related to the quality and quantity of struvite product. Although induced hydrothermal precipitation in the synthetic MAP solution could be reached in the reasonable quantities (90 wt%) of struvite, struvite production was constrained by the existing of Ca^{2+}/HCO^{-}_{3} ions in the hydrothermal solution, in which the struvite product rarely exceeded 50 cwt. % after 1 h of experiments. Correspondingly, the concentration of Ca^{2+} and PO^{3-}_{4} is higher than O^{2-} and Mg^{2+} in the hydrothermal solution made some insoluble calcium phosphate (e.g. hydroxyapatite and Mg-whitlockite) to precipitate (Ahn and Speece, 2006). Comparing with data in the literature showed that struvite and calcium phosphate compounds observed here can be similar, while more crystalline phases than the amorphous phase can be produced in the study (Liu and Wang, 2019).

In the present study, struvite purity, as presented XRPD phase fraction, could be produced from the synthetic wastewater solution, whereas the real wastewater having varying chemical compositions that can make grown many minerals (e.g. calcite, hydroxyapatite, and dolomite) simultaneously during struvite crystallization (Liu and Wang, 2019; Yan and Shih, 2016). Accordingly, the presence of competitive ions (e.g. Ca^{2+} and HCO^{-}_{3}-ions) leads to a result in reducing struvite's purity with the growth of the undesired minerals. For instance, the dairy wastewater has been always rich in calcium, therefore the hydrothermal treatment of this wastewater may produce more hydroxyapatite than struvite, which has an impact on reducing the struvite product as a slow-release phosphate fertilizer (Daneshgar et al., 2018). Additionally, hydroxyapatite is not recommended for use as a fertilizer, because it causes soil with a low phosphate activity and high salt concentration.

Further significant results presented in the study related to simulation on the biomineralization of carbonate and phosphate using the hydrothermal solution with varying $Mg^{2+}/Ca^{2+}/HCO^{-}_{3}$ molar ratios. Hydroxyapatite, Mg-whitlockite, and struvite were precipitated in variable proportions depending on variable $Mg^{2+}/Ca^{2+}/HCO^{-}_{3}$ molar ratios of the medium. In particular, Mg-whitlockite is a calcium orthophosphate crystal in which magnesium partly substitutes for calcium. Interestingly, Mg-whitlockite constitutes a biomineral in living bone (Lagier and Baud, 2003), whereas the synthesis of this single-phase mineral still remains a challenge. Accordingly, biomineralization through the hydrothermal process of wastewater may produce carbonate and phosphate

Table 3
XRPD mineralogy of hydrothermal products.

Hydrothermal operating condition	Mineral	pH solution of 9 (wt. %)	pH solution of 10 (wt. %)	pKps
120/24 h	Struvite	91.83(0.13)[a]	88.48 (0.22)	13.17
MAP ratio of (1:1:1)	Dittmarite	4.47 (0.42)	9.96 (0.54)	n/a
	Sylvite	3.70 (0.36)	1.56 (0.17)	−0.85
120/24 h	Struvite	1.64 (0.14)	12.64 (0.68)	13.17
Mg:Ca:HCO_3 ratio of (1:1:1)	Hydroxyapatite	14.26 (0.62)	76.34 (0.73)	54.45
	Mg-whitlockite	26.50 (0.90)	6.67 (0.52)	28.88
	Dolomite	56.72 (0.17)	0.90 (0.21)	17.09
	Calcite	0.65 (0.09)	3.16 (0.9)	8.48
	Sylvite	0.23 (0.04)	0.29 (0.09)	−0.85
120/24 h				
Mg:Ca:HCO_3 ratio	Struvite	10.94 (0.15)		13.17
(2:1:1)	Hydroxyapatite	61.92 (0.29)	63.11 (0.14)	54.45
	Calcite	22.09 (0.37)	21.75 (0.73)	8.48
	Sylvite	5.05 (0.11)	15.13 (0.49)	−0.85
Mg:Ca:HCO_3 ratio (1:2:2)	Mg-whitlockite	48.10 (0.20)		28.88
	Hydroxyapatite	37.54 (0.61)	81.69 (0.71)	54.45
	Calcite	5.84(0.21)	18.31 (0.21)	8.48
	Sylvite	8.52(0.43)		−0.85

[a] Number in the bracket represents the standard deviation of the value. n/a = not available.

minerals, which require control of ionic composition and concentration of the solution (Li et al., 2009, 2017). It has demonstrated during the study that achievement for pure struvite precipitation relates to initial concentrations of MAP components, pH value and in the absence of the competitive ions (e.g. Ca and HCO_3-ions). Subsequent adding of the inorganic components (e.g $Mg^{2+}/Ca^{2+}/HCO^{-}_3$) made the hydrothermal solution changed into typical for the wastewater of the Ca–PO_4 system tending to the crystallization of the calcium phosphates (e.g. hydroxyapatite, Mg-whitlockite). The increasing pH values lead to the biomineralization process of calcium phosphates (Liu and Wang, 2019; Yan and Shih, 2016). Therefore the control strategy of Ca^{2+}/HCO^{-}_3 ions present in the MAP solution through proposed different steps of wastewater treatment should be adopted for producing a minimum level of these ions which insignificant influence on the struvite crystallization (Liu and Wang, 2019).

Regarding whitlockite versus hydroxyapatite, only a few studies can be found in the literature, in that evolution of those minerals could be linked to a living process in biology and pathology (Lagier and Baud, 2003). It was suggested that whitlockite and hydroxyapatite could be formed together in an aqueous system at a temperature compatible with biological conditions. Therefore, they may be formed in the hydrothermal condition (Li et al., 2017). In this study, hydrothermal synthesis of the MAP solution with varying $Mg^{2+}/Ca^{2+}/HCO^{-}_3$ molar ratios at 120 ^{O}C provided direct experimental evidence of whitlockite and hydroxyapatite formed in the precipitating products, as the finding was confirmed by XRD Rietveld method in agreement with the crystal structure database (Downs and Hall-Wallace, 2003). Still, much work need to be done for finding a crystallization mechanism of those minerals.

4. Conclusion

The impact of variable $Mg^{2+}/Ca^{2+}/HCO^{-}_3$ molar ratios on the hydrothermal crystallization of struvite has been examined by XRPD and SEM analysis. In the absence of these ions, the hydrothermal solution yielded struvite and dittmarite crystals at pH values (9 and 10) and the constant temperature of 120 ^{O}C. However, the struvite crystallization has been hindered by the presence of competing ions ($Mg^{2+}/Ca^{2+}/HCO^{-}_3$) yielding to a lower proportion of struvite. Correspondingly, the formation of an amorphous substance and other crystalline phases (e.q. calcite, hydroxyapatite, and Mg-whitlockite) occurred in the hydrothermal solution, depending on varying $Mg^{2+}/Ca^{2+}/HCO^{-}_3$ molar ratios and pH. The results revealed the low proportion of struvite for experiments with $Mg^{2+}/Ca^{2+}/HCO^{-}_3$ molar ratios may be a limitation of the struvite tendency for phosphate recovery.

Statement of author contribution

B.A.P and S.W.W designed the experiments. B.A.P prepared the solution and carried out crystallization experiments. B.A.P carried out Rietveld analysis of XRD data and SEM studies. B.A.P and S.W.W Prepared and finally approved for the version to be published the manuscript.

Acknowledgments

The study was supported by the KAAD (*Katholischer Akademischer Austausch Dienst*) Bonn and Diponegoro University (UNDIP) under World Class University (WCU) Professor sabbatical program at LMU Munich 2019. The assistance of Dr. Erika Griesshaber in collecting electron microscope analysis data is appreciated. The Author thank to Miss. Stefanie Hoser performing laboratory experiments.

References

Abbona, F., Madsen, H.E.L., Boistelle, R., 1986. The initial phases of calcium and magnesium phosphates precipitated from solutions of high to medium concentrations. J. Cryst. Growth 74, 581–590.
Ahn, Y.H., Speece, R.E., 2006. Waste lime as a potential cation source in the phosphate crystallization process. Environ. Technol. 27 (11), 1225–1231.
Ajikumar, P.K., Wong, L.G., Subramanyam, G., Lakshminarayanan, R., Valiyaveettil, S., 2005. Synthesis and characterization of mono dispersed spheres of amorphous calcium carbonate and calcite spherules. Cryst. Growth Des. 5, 1129–1134.
Babic-Ivancic, V., Kontrec, J., Brečević, L., Kralj, D., 2006. Kinetics of struvite to newberyite transformation in the precipitation system $MgCl_2$–$NH_4H_2PO_4$–NaOH–H_2O. Water Res. 40, 3447–3455.
Bayuseno, A.P., Schmahl, W.W., 2018. Hydrothermal synthesis of struvite and its phase transition: impacts of pH, heating and subsequent cooling methods. J. Cryst. Growth 498, 336–345.
Bayuseno, A.P., Schmahl, W.W., 2019. Thermal decomposition of struvite in water: qualitative and quantitative mineralogy analysis. Environ. Technol. 1–7.
Bhuiyan, M.I.H., Mavinic, D.S., Beckie, R.D., 2007. A solubility and thermodynamic study of struvite. Environ. Technol. 28, 1015–1026.
Bhuiyan, M.I.H., Mavinic, D.S., Koch, F.A., 2008. Thermal decomposition of struvite and its phase transition. Chemosphere 70, 1347–1356.
Booker, N.A., Priestley, A.J., Fraser, I.H., 1999. Struvite formation in wastewater treatment plants: opportunities for nutrient recovery. Environ. Technol. 20, 777–782.
Bouropoulos, N.C., Koutsoukos, P.G., 2000. Spontaneous precipitation of struvite from aqueous solutions. J. Cryst. Growth 213, 381–388.
Capdevielle, A., Sykorová, E., Biscans, B., Béline, F., Daumer, M.-L., 2013. Optimization of struvite precipitation in synthetic biologically treated swine wastewater-Determination of the optimal process parameters. J. Hazard Mater. 244–245, 357–369.
Daneshgar, S., Buttafava, A., Capsoni, D., Callegari, A., Capodaglio, A.G., 2018. Impact of pH and ionic molar ratios on phosphorous forms precipitation and recovery from different wastewater sludges. Resources 7, 71.
de-Bashan, L.E., Bashan, Y., 2004. Recent advances in removing phosphorus from wastewater and its future use as fertilizer (1997–2003). Water Res. 38, 4222–4246.
Downs, R.T., Hall-Wallace, M., 2003. The American Mineralogist crystal structure database. Am. Mineral. 88, 247–250.
Doyle, J.D., Parsons, S.A., 2002. Struvite formation, control and recovery. Water Res. 36, 3925–3940.
Doyle, J.D., Oldring, K., Churchley, J., Parsons, S.A., 2002. Struvite formation and the fouling propensity of different materials. Water Res. 36, 3971–3978.
Doyle, J.D., Oldring, K., Churchley, J., Price, C., Parsons, S.A., 2003. Chemical control of struvite precipitation. J Environ Eng. – ASCE 129, 419–426.
Durrant, A.E., Scrimshaw, M.D., Stratful, I., Lester, J.N., 1999. Review of the feasability of recovering phosphate from wastewater for use as a raw material by the phosphate industry. Environ. Technol. 20, 749–758.
Elliott, D.C., Biller, P., Ross, A.B., Schmidt, A.J., Jones, S.B., 2015. Review-Hydrothermal liquefaction of biomass: developments from batch to continuous process. Bioresour. Technol. 178, 147–156.
Gaterell, M.R., Gay, R., Wilson, R., Gochin, R.J., Lester, J.N., 2000. An economic and environmental evaluation of the opportunities for substituting phosphorus recovered from wastewater treatment works in existing UK fertilizer markets. Environ. Technol. 21, 1067–1084.
Hanhoun, M., Montastruc, L., Azzaro-Pantel, C., Biscans, B., Frèche, M., Pibouleau, L., 2011. Temperature impact assessment on struvite solubility product: a thermodynamic modeling approach. Chem. Eng. J. 167, 50–58.
Hii, K., Baroutian, S., Parthasarathy, R., Gapes, D.J., Eshtiaghi, N., 2014. A review of wet air oxidation and thermal hydrolysis technologies in sludge treatment. Bioresour. Technol. 155, 289–299.
Jesse, S.D., Davidson, P.C., 2019. Treatment of post-hydrothermal liquefaction wastewater (PHWW) for heavy metals, nutrients, and indicator pathogens. Water 11, 854.
Kofina, A.N., Demadis, K.D., Koutsoukos, P.D., 2007. The Effect of citrate and phosphocitrate on struvite spontaneous precipitation. Cryst. Growth Des. 7, 2705–2712.
Kofina, A.N., Koutsoukos, P.G., 2003. Nucleation and crystal growth of struvite in aqueous media. New prospectives in phosphorus recovery. In: Wasic Workshop, Istanbul (Turkey).
Kontrec, J., Babič-Ivancić, V., Brecević, L., 2005. Formation and Morphology of Struvite and Newberyite in Aqueous Solutions at 25 and 37 °C. Coll. Antropol. 29, 289–294.
Korchef, A., Saidou, H., Amor, M.B., 2011. Phosphate recovery through struvite precipitation by CO_2 removal: effect of magnesium, phosphate and ammonium concentrations. J. Hazard Mater. 86, 602–613.
Lagier, R., Baud, C.-A., 2003. Magnesium whitlockite, a calcium phosphate crystal of special interest in Pathology. Pathol. Res. Pract. 199, 329–335.
Le Corre, K.S., Valsami-Jones, E., Hobbs, P., Parsons, S.A., 2005. Impact of calcium on struvite crystal size, shape and purity. J. Cryst. Growth 283, 514–522.
Li, X., Ito, A., Sogo, Y., Wang, X., Le Geros, R.Z., 2009. Solubility of Mg-containing β-tricalcium phosphate at 25 °C. Acta Biomater. 5, 508–517.
Li, G.-C., Wang, P., Liu, C.-B., 2017. Hydrothermal synthesis of whitlockite. J. Inorg. Mater. 32, 1128–1132.

Li, B., Boiarkina, I., Yu, W., Huang, H.M., Munir, T., Wang, G.Q., Young, B.R., 2019. Review-Phosphorous recovery through struvite crystallization: challenges for future design. Sci. Total Environ. 648, 1244–1256.
Liu, X., Wang, J., 2019. Impact of calcium on struvite crystallization in the waste water and its competition with magnesium. Chem. Eng. J. 378, 122121–122123.
Lu, X., Shih, K., Li, X.-Y., Liu, G., Zeng, E.Y., Wang, F., 2016. Accuracy and application of quantitative X-ray diffraction on the precipitation of struvite product. Water Res. 90, 9–14.
Mahieux, P.-Y., Aubert, J.-E., Cyr, M., Coutand, M., Husson, B., 2010. Quantitative mineralogical composition of complex mineral wastes–contribution of the Rietveld method. Waste Manag. 30, 378–388.
Mamais, D., Pitt, P.A., Cheng, Y.W., Loiacono, J., Jenkins, D., Wen, Y., 2012. Digesters determination to control in anaerobic of ferric chloride precipitation digesters dose struvite sludge. Water Environ. Res. 66, 912–918.
McMillen, C.D., Kolis, J.W., 2016. Hydrothermal synthesis as a route to mineralogically-inspired structures. Dalton Trans. 45, 2772–2784.
Mohajit, X., Bhattarai, K.K., Taiganides, E.P., Yap, B.C., 1989. Struvite deposits in pipes and aerators. Biol. Waste 30, 133–147.
Montes, F., Rotz, C.A., Chaoui, H., 2009. Process modeling of ammonia volatilization from ammonium solution and manure surfaces: a review with recommended models. Trans. ASABE (Am. Soc. Agric. Biol. Eng.) 52, 1707–1719.
Munir, M.T., Li, B., Boiarkina, I., Baroutian, S., Yu, W., Young, B.R., 2017. Phosphate recovery from hydrothermally treated sewage sludge using struvite precipitation. Bioresour. Technol. 239, 171–179.
Muryanto, S., Bayuseno, A.P., 2014. Influence of Cu^{2+} and Zn^{2+} as additives on precipitation kinetics and morphology of struvite. Powder Technol. 253, 602–607.
Musvoto, E., Wentzel, M., Loewenthal, R., Ekama, G., 2000a. Integrated chemical-physical processes modelling-I. Development of a kinetic-based model for mixed weak acid/base systems. Water Res. 34, 1857–1867.
Musvoto, E.V., Wentzel, M.C.M., Ekama, G.A.M., 2000b. Integrated chemical—physical processes modelling II. Simulating aeration treatment of anaerobic digester Supernatants. Water Res. 34, 1868–1880.
Ohlinger, K.N., Young, T.M., Schroeder, E.D., 1999. Kinetics effects on preferential struvite accumulation in waste-water. J. Environ. Eng. 125, 730–737.
Ohlinger, K.N., Young, T.M., Schroeder, E.D., 2000. Postdigestion struvite precipitation using a fluidized bed reactor. J. Environ. Eng. 126, 361–368.
Parkhurst, D.L., Appelo, C.A.J., 1999. User's Guide to PHREEQC (Version 2), a Computer Program for Speciation, Batch-Reaction, One-Dimensional Transport and Inverse Geochemical Calculations. USGS Water-Resources Investigations Report, pp. 99–4259.
Perwitasari, D.S., Edahwati, L., Sutiyono, S., Muryanto, S., Jamari, J., Bayuseno, A.P., 2017. Phosphate recovery through struvite-family crystals precipitated in the presence of citric acid: mineralogical phase and morphology evaluation. Environ. Technol. 38, 2844–2855.
Rahman, Md M., Salleh, M.A.M., Rashid, K., Ahsan, A., Hossain, M.M., Ra, C.S., 2014. Production of slow release crystal fertilizer from wastewaters through struvite crystallization – a review. Arab. J. Chem. 7, 139–155.
Rawn, A.M., Perry, Banta A., Pomeroy, R., 1937. Multiple-stage Sewage Sludge Digestion. American Society of Civil Engineers, pp. 93–132.
Reißmann, D., Thrän, D., Bezama, A., 2018. How to identify suitable ways for the hydrothermal treatment of wet bio-waste? A critical review and methods proposal. Waste Manag. Res. 36, 912–923.
Rietveld, H.M., 1969. A profile refinement method for nuclear and magnetic structures. J. Appl. Crystallogr. 2, 65–71.
Rodriguez-Carvajal, J., June 2005. Program Fullprof.2k, Version 3.30. Laboratoire Leon Brillouin, France.
Sartorius, C., von Horn, J., Tettenborn, F., 2011. Phosphorus recovery from wastewater–state-of-the-art and future potential. Proc. Water Environ. Federation 1, 299–316.
Shanmugam, S.R., Adhikari, S., Shakya, R., 2017. Nutrient removal and energy production from aqueous phase of bio-oil generated via hydrothermal liquefaction of algae. Bioresour. Technol. 230, 43–48.
Shu, L., Schneider, P., Jegatheesan, V., Johnson, J., 2006. An economic evaluation of phosphorus recovery as struvite from digester supernatant. Bioresour. Technol. 97, 2211–2216.
Snoeyink, V.L., Jenkins, D., 1980. Water Chemistry. John Wiley and sons, New York.
Song, Y., Qian, F., Gao, Y., Huang, X., Wu, J., Yu, H., 2015. PHREEQC program-based simulation of magnesium phosphates crystallization for phosphorus recovery. Environ. Earth Sci. 73, 5075–5084.
Stratful, I., Scrimshaw, M.D., Lester, J.N., 2001. Conditions influencing the precipitation of magnesium ammmonium phosphate. Water Res. 35, 4191–4199.
Stum, W., Morgan, J.J., 1970. Aquatic Chemistry. Wiley-Intersecience, New York, NY, p. 583.
Talboys, P.J., Heppell, J., Roose, T., Healey, J.R., Jones, D.L., Withers, P.J.A., 2016. Struvite: a slow-release fertiliser for sustainable phosphorus management? Plant Soil 401, 109–123.
Tansel, B., Lunn, G., Monje, O., 2018. Review: struvite formation and decomposition characteristics for ammonia and phosphorus recovery: a review of magnesium-ammonia phosphate interactions. Chemosphere 194, 504–514.
Williams, S., 1998. Struvite precipitation in the sludge treatment stream at Slough wastewater treatment plant and opportunities for phosphorus recovery. Environ. Technol. 20, 743–747.
Winburn, R.S., Grier, D.G., McCarthy, G.J., Peterson, R.B., 2000. Rietveld quantitative X-ray diffraction analysis of NIST fly ash standard reference materials. Powder Diffr. 15, 163–172.
Xue, X., Chen, D., Song, X., Dai, X., 2015. Hydrothermal and pyrolysis treatment for sewage sludge: choice from product and from energy benefit. Energy Procedia 66, 301–304.
Yan, H., Shih, K., 2016. Effects of calcium and ferric ions on struvite precipitation: a new assessment based on quantitative X-ray diffraction analysis. Water Res. 95, 310–318.
Zhu, Y., Wei, J., Liu, Y., Liu, X., Li, J., Zhang, J., 2019. Assessing the effect on the generation of environmentally persistent free radicals in hydrothermal carbonization of sewage sludge. Sci. Rep. 9, 17092.

Crystallization of struvite in a hydrothermal solution with and without calcium and carbonate ions

ORIGINALITY REPORT

9%	6%	7%	2%
SIMILARITY INDEX	INTERNET SOURCES	PUBLICATIONS	STUDENT PAPERS

PRIMARY SOURCES

1	Xiangyu Xue, Dezhen Chen, Xueding Song, Xiaohu Dai. "Hydrothermal and Pyrolysis Treatment for Sewage Sludge: Choice from Product and from Energy Benefit1", Energy Procedia, 2015 Publication	<1%
2	www.mdpi.com Internet Source	<1%
3	worldwidescience.org Internet Source	<1%
4	Lu, Xingwen, Kaimin Shih, Xiao-yan Li, Guoqiang Liu, Eddy Y. Zeng, and Fei Wang. "Accuracy and application of quantitative X-ray diffraction on the precipitation of struvite product", Water Research, 2016. Publication	<1%
5	Submitted to The University of the South Pacific Student Paper	<1%
	www.iasj.net	

6	Internet Source	<1%
7	M. Iqbal H. Bhuiyan, D.S. Mavinic, F.A. Koch. "Thermal decomposition of struvite and its phase transition", Chemosphere, 2008 Publication	<1%
8	www.nature.com Internet Source	<1%
9	thesis.library.caltech.edu Internet Source	<1%
10	www.intechopen.com Internet Source	<1%
11	Bhuiyan, M.I.H.. "Thermal decomposition of struvite and its phase transition", Chemosphere, 200802 Publication	<1%
12	Xuewei Li, Xiaowen Zhou, Bo Yang, Zhen Wena. "Recovery phosphate and ammonium from aqueous solution by the process of electrochemically decomposing dolomite", Chemosphere, 2021 Publication	<1%
13	Chathurani Moragaspitiya, Jay Rajapakse, Graeme J. Millar. "Effect of struvite and organic acids on immobilization of copper and zinc in contaminated bio-retention filter	<1%

media", Journal of Environmental Sciences, 2020
Publication

14	Submitted to Grand Canyon University Student Paper	<1 %
15	sphinxsai.com Internet Source	<1 %
16	www.aqion.de Internet Source	<1 %
17	S. Sutiyono, Luluk Edahwati, Dyah Suci Perwitasari, Stefanus Muryanto, J. Jamari, Anatasius P. Bayuseno. "Synthesis and Characterisation of Struvite Family Crystals by An Aqueous Precipitation Method", MATEC Web of Conferences, 2016 Publication	<1 %
18	Mehta, Chirag M., and Damien J. Batstone. "Nutrient solubilization and its availability following anaerobic digestion", Water Science & Technology, 2013. Publication	<1 %
19	escholarship.org Internet Source	<1 %
20	Bing Li, Irina Boiarkina, Wei Yu, Hai Ming Huang, Tajammal Munir, Guang Qian Wang, Brent R. Young. "Phosphorous recovery through struvite crystallization: Challenges for	<1 %

future design", Science of The Total Environment, 2019
Publication

21	Haiming Huang. "Recovery of nitrogen from saponification wastewater by struvite precipitation", Water Science & Technology, 08/2010 Publication	<1 %
22	Submitted to University of Massachusetts - Amherst Student Paper	<1 %
23	Yongmei Li, Jinte Zou, Lili Zhang, Jing Sun. "Aerobic granular sludge for simultaneous accumulation of mineral phosphorus and removal of nitrogen via nitrite in wastewater", Bioresource Technology, 2014 Publication	<1 %
24	L. Edahwati, S. Sutiyono, S. Muryanto, J. Jamari, A. P. Bayuseno. "Optimized Phosphate Recovery Through MAP Precipitation in an Air Agitated Column Reactor", Oriental Journal of Chemistry, 2018 Publication	<1 %
25	agupubs.onlinelibrary.wiley.com Internet Source	<1 %
26	polen.itu.edu.tr Internet Source	<1 %

27	José Luis Campos, Dafne Crutchik, Óscar Franchi, Juan Pablo Pavissich et al. "Nitrogen and Phosphorus Recovery From Anaerobically Pretreated Agro-Food Wastes: A Review", Frontiers in Sustainable Food Systems, 2019 Publication	<1 %
28	Sheik, Abdul R., Emilie E. L. Muller, and Paul Wilmes. "A hundred years of activated sludge: time for a rethink", Frontiers in Microbiology, 2014. Publication	<1 %
29	e-collection.library.ethz.ch Internet Source	<1 %
30	www.science.gov Internet Source	<1 %
31	Vesna Babić-Ivančić, Jasminka Kontrec, Ljerka Brečević, Damir Kralj. "Kinetics of struvite to newberyite transformation in the precipitation system MgCl2–NH4H2PO4–NaOH–H2O", Water Research, 2006 Publication	<1 %
32	Y.D. Yilmazel, G.N. Demirer. "Removal and recovery of nutrients as struvite from anaerobic digestion residues of poultry manure", Environmental Technology, 2011 Publication	<1 %
	dgk-home.de	

33	Internet Source	<1%
34	dokumen.pub Internet Source	<1%
35	edoc.hu-berlin.de Internet Source	<1%
36	iwaponline.com Internet Source	<1%
37	library.naturalsciences.be Internet Source	<1%
38	sfamjournals.onlinelibrary.wiley.com Internet Source	<1%
39	www.geochemicalperspectivesletters.org Internet Source	<1%
40	Babaie, Elham, Huan Zhou, Boren Lin, and Sarit B. Bhaduri. "Influence of ethanol content in the precipitation medium on the composition, structure and reactivity of magnesium–calcium phosphate", Materials Science and Engineering C, 2015. Publication	<1%
41	Kumar, M.. "Beneficial phosphate recovery from reverse osmosis (RO) concentrate of an integrated membrane system using polymeric ligand exchanger (PLE)", Water Research, 200705	<1%

Publication

42	Milan Malhotra, Anurag Garg. "Hydrothermal carbonization of centrifuged sewage sludge: Determination of resource recovery from liquid fraction and thermal behaviour of hydrochar", Waste Management, 2020 Publication	<1 %
43	Nadja Zupan Hajna, Roman Skála, Asma Al-Farraj, Martin Šťastný, Pavel Bosák. "Palygorskite from cave sediments: case study from Wadi Haqil, United Arab Emirates", Arabian Journal of Geosciences, 2016 Publication	<1 %
44	epubs.surrey.ac.uk Internet Source	<1 %
45	rasayanjournal.co.in Internet Source	<1 %
46	www.phosphatefacts.com Internet Source	<1 %
47	www.scribd.com Internet Source	<1 %
48	Juan Diego Rodriguez-Blanco, Samuel Shaw, Pieter Bots, Teresa Roncal-Herrero, Liane G. Benning. "The role of Mg in the crystallization of monohydrocalcite", Geochimica et Cosmochimica Acta, 2014 Publication	<1 %

49	Crutchik, D., A. Sánchez, and J.M. Garrido. "Simulation and experimental validation of multiple phosphate precipitates in a saline industrial wastewater", Separation and Purification Technology, 2013. Publication	<1%
50	digitalscholarship.unlv.edu Internet Source	<1%
51	iahr.tandfonline.com.tandf-prod.literatumonline.com Internet Source	<1%

Exclude quotes	Off	Exclude matches	Off
Exclude bibliography	On		

Crystallization of struvite in a hydrothermal solution with and without calcium and carbonate ions

GRADEMARK REPORT

FINAL GRADE

/0

GENERAL COMMENTS

Instructor

PAGE 1

PAGE 2

PAGE 3

PAGE 4

PAGE 5

PAGE 6

PAGE 7

PAGE 8

PAGE 9

PAGE 10